

# THE APPLICATION OF POINT SPREAD FUNCTION WEIGHTING IN PROBABILISTIC TRACTOGRAPHY

D. M. Morris<sup>1</sup>, S. Zhao<sup>1</sup>, and G. J. Parker<sup>1</sup>

<sup>1</sup>Imaging Science and Biomedical Engineering, University of Manchester, Manchester, United Kingdom

**Background** – Probabilistic tractography has been developed for the non invasive assessment of confidence that may be given to cerebral anatomical connections[1,2]. These are identified by fibre tracking algorithms applied to diffusion weighted images (DWI). The Monte Carlo streamline processes used are based on the sampling of probability density functions (PDFs) which define the distribution of fibre orientations determined from the DWI at a voxel level. Interpolation of PDFs between voxels generally follows the proposal of Behrens et al [3], who suggested random sampling of neighbourhood PDFs, weighted according to the distance of the point under consideration from the neighbourhood voxel centres (Fig. 1). Over many Monte Carlo this results in tri-linear interpolation, giving linear weightings with distance of the streamline from the neighbouring PDFs in the x, y and z directions. Whilst tri-linear weighting is the simplest scheme for sampling neighbouring PDFs it does not take into account the presence of the voxel point spread function (PSF), which affects the way that signals from each of the neighbouring voxels are distributed in space. Here we investigate whether using more realistic weighting functions and PDF selection has a significant effect on PDF selection for probabilistic tractography.

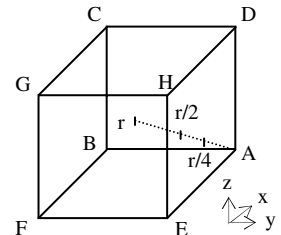


Figure 1 – Streamline positions relative to the neighbouring PDFs A-H

**Methods** – The PSF varies according to imaging protocol implementation. A protocol routinely used for evaluating neuroanatomical connections was assessed: 3T Philips Achieva scanner using SE EPI  $TE = 54$  ms,  $TR = 11884$  ms,  $G = 62$  mTm<sup>-1</sup>, phase encoding left-right,  $112 \times 112$  matrix, SENSE factor 2.5, reconstructed resolution 1.88 mm, slice thickness 2.1 mm, 60 slices, 61 diffusion sensitisation directions at  $b = 1200$  smm<sup>-2</sup> ( $\Delta, \delta = 28.5, 13.5$  ms), and 1  $b = 0$  image. The in-plane PSF is assumed to be generated only by the truncation and sampling of the continuous MRI signal in k-space. With knowledge of the physical image dimensions and the sampling interval employed, the periodicity of the resulting sinc-shaped PSF can be analytically determined [4], the FWHM of the central lobe being equal to a factor 1.21 of the pixel dimensions. The true in-plane point spread function will additionally include contributions due to  $T_2^*$  decay which will be variable across the brain but these were not assessed in this initial study. The through-plane PSF can be determined by estimation of the slice profile, which was calculated by numerical differentiation of a wedge phantom profile [5]. This is approximated as a Gaussian profile with a FWHM of approximately the slice thickness. Whilst the weighting function from the PSF will extend beyond these nearest neighbour voxels, we have restricted the weighting to within a single voxel to allow direct comparison between the nearest neighbours under different weighting regimes. Normalisation of the x, y, and z PSFs is carried out to give a total PSF weighting of unity in x, y and z. To compare the differences caused by using PSF based weighting as opposed to the current linear, the probability of selecting from the PDFs A-H was compared. The weighting values were compared for a streamline positioned half the distance toward PDF A from the centre ( $r/2$ ) and half that distance again ( $r/4$ ) (Fig. 1).

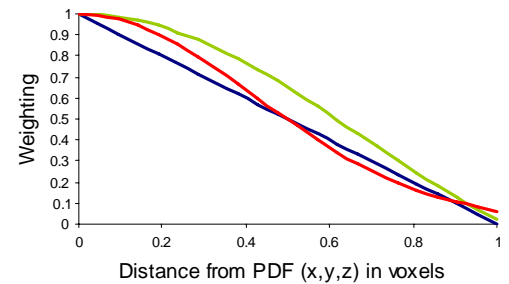


Figure 2 – Weighting functions at different distances from the defined PDFs (x&y) Red and (z) Green. Linear weighting shown in Blue

**Results** – The PSF weighting functions for the different distances from the PDFs can be seen in Fig.2 for in-plane (x,y) and through-plane (z) along with the weightings provided by linear weighting for comparison. In Fig.3 the probability of each of the eight possible PDFs being selected is displayed for the positions  $r/2$  and  $r/4$  for the linear and PSF-based weightings. These differences, when using PSF as opposed to linear weighting, are collated in Fig. 4 as the absolute change/percentage change in the probability of a particular PDF being selected.

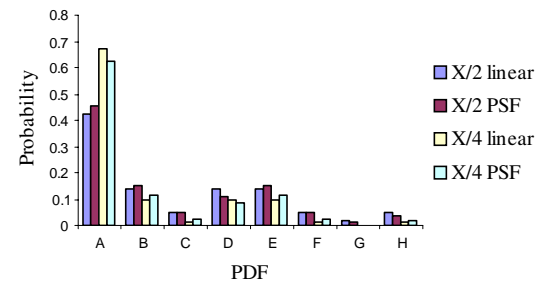


Figure 3 – Probability of PDF selection depending on streamline position ( $r/2$  or  $r/4$ ) and weighting (linear or PSF)

**Discussion and conclusion** – The use of the PSF to weight the selection of PDFs in probabilistic tractography leads to measurable changes from linear weighting. The changes in the probability of selecting a particular PDF with the non-linear weighting varies between the in-plane and through-plane directions. Whilst in general the increase in weighting close to the PDFs will increase the probability of sampling the nearest PDF, this may be counteracted by the decreased weightings at distance. This interaction will depend on the form of the weighting function. This simple implementation has shown that the use of PSF-based weighting functions can affect the probability of PDF selection. These effects will increase with more rigorous treatment as the weighting functions are applied outside the nearest neighbour PDFs and with PSFs including the affects of  $T_2^*$  during image capture. This has the potential to significantly influence the probabilistic tracking profiles derived depending on the local variability of the area being tracked through.

PDF	Position $r/2$	Position $r/4$
A	0.0339/8.04%	-0.0449/-6.70%
B	0.0096/6.85%	0.0203/21.19%
C	0.0027/5.67%	0.0079/51.42%
D	-0.0308/-21.90%	-0.0093/-9.68%
E	0.0096/6.85%	0.0203/21.19%
F	0.0027/5.67%	0.0079/57.42%
G	-0.0037/-23.61%	0.0010/52.40%
H	-0.0107/-22.76%	0.0024/17.32%

Figure 4 – Absolute and Percentage change in probability of a PDF being selected using PSF and linear weighting

**References** – [1] Parker, G.J. and D.C. Alexander. Lect. Notes Comp. Sci., 2003. 2737: p. 684-695. [2] Parker, G. J. M. and D. C. Alexander. Phil. Trans. Roy. Soc. Series B, 2005. 360: p. 893-902.[3] Behrens TEJ, et al. MRM 20003. 50(5):p 1077-1088 [4]Haacke et al eds. Magnetic Resonance Imaging: Physical Principle and Sequence Design John Wiley and Sons, New York:1999 [5] Lerski R et al . Quality control in magnetic resonance imaging. Report 80. IPEM York: 2000.

**Acknowledgements** – This work was funded by the Engineering and Physical Sciences Research Council (EPSRC) UK through Grant GR/T02669/01.